

Investigation of mechanical properties of ϵ -zirconium hydride using micro- and nano-indentation techniques

Jiujun Xu ^{a,b}, San-Qiang Shi ^{b,*}

^a Institute of Materials and Technology, Dalian Maritime University, 116026 Dalian, China

^b Department of Mechanical Engineering, The Hong Kong Polytechnic University, Hung Hom, Kowloon, Hong Kong, China

Received 3 February 2003; accepted 3 February 2004

Abstract

Mechanical properties of metal hydrides are difficult to measure because of the difficulties in making flaw-free macro-size specimens. Nano-indentation and micro-indentation techniques were used in this report to study mechanical properties of zirconium hydrides ($ZrH_{1.83}$). Hardness, apparent Young's modulus, yield stress and fracture toughness of zirconium hydrides were measured and compared to the values for a zirconium sample.

© 2004 Elsevier B.V. All rights reserved.

PACS: 81.05.Je; 46.50.+a; 81.40.Np; 83.60.La

1. Introduction

Hydride embrittlement in zirconium and its alloys is a concern in nuclear power industry. Since these alloys are working under hot water environment, hydrogen can penetrate into these alloys through corrosion process. When hydrogen concentration reaches solubility limit, hydrides will form and can cause mechanical failure under certain circumstances. Three types of hydrides, γ , δ and ϵ , can form in zirconium–hydrogen system. It is critical to know the mechanical properties of zirconium hydrides. Early studies were made using conventional mechanical testing methods. Tensile tests on pure zirconium hydrides [1] indicated zero ductility at temperatures up to 600 °C. Barraclough and Beevers [2,3] also reported zero ductility in tensile tests on pure hydrides up to 500 °C with a maximum fracture stress of about 70 MPa, but δ , ($\gamma + \delta$) and ϵ -hydrides were deformable in compression above 100 °C with a maximum fracture

stress of 225 MPa. Micro-hardness tests [4] on solid hydride layers also indicated similar behavior. Delayed hydride cracking (DHC) tests [5–7] showed that brittle fracture of hydrides at crack tip occurred at temperatures at least as high as 300 °C. Fracture toughness tests by Simpson and Cann on pure hydride [8] revealed low fracture toughness of 0.5–5 MPa m^{1/2} for δ -hydrides in temperatures up to 400 °C. However, it is known that large pieces of zirconium hydrides may contain defects such as voids and micro-cracks due to a large volume expansion during hydride formation (e.g., volume of δ -hydride phase is about 17% larger than the original zirconium matrix). Therefore it is questionable whether or not the mechanical strength measured using macro-size pure hydrides is reliable. Acoustic emission technique was applied recently on zirconium specimens containing 100 ppm by weight of hydrogen [9]. It was assumed that the hydride formed inside zirconium matrix has less crack-like defects. Results from this test showed that the fracture strength of hydrides in zirconium matrix was about 650 MPa up to 140 °C and has a weak dependence on temperature. On the other hand, the yield strength of zirconium matrix decreases quickly as temperature increases, resulting in flow of hydride particles with the deforming zirconium at higher

* Corresponding author. Tel.: +852-2766-7821; fax: +852-2365-4703.

E-mail address: mmsqshi@polyu.edu.hk (S.-Q. Shi).

temperatures [9]. A recent study [10,11] showed unusually high values of Young's modulus by measuring sound velocities in hydrides and high values of Vickers hardness in the composition range of $ZrH_{1.5}$ – $ZrH_{1.7}$. These values are much higher than those values for a zirconium metal. A micro-hardness study revealed significant reductions of these properties and yield strength of hydrides at higher hydrogen contents [12].

In recent years, theoretical modeling of hydride embrittlement in zirconium alloys has made significant progresses [13–20]. Most of the modeling works were based on Eshalby's inclusion theory [21], in which, a hydride was treated as an inclusion having elastic misfit strains with the matrix. However, because of the lack of experimental data on mechanical properties of the hydrides, all theories so far have assumed that the hydrides have the same elastic properties as for zirconium. In this article, we report the experimental investigation using modern nano-indentation technology on a solid hydride ($ZrH_{1.83}$) and a zirconium metal, to measure the elastic modulus, yield stress and hardness of the hydrides. The advantage of nano-indentation technique is to measure mechanical properties of hydrides in small scale in order to avoid the defected zones in a macro-size specimen. We also applied micro-hardness technique to measure the fracture toughness of zirconium hydrides.

2. Experimental procedures

2.1. Specimen preparation

A reactor grade zirconium plate was used in this work. Hydriding was carried out gaseously in a glass system with purified hydrogen gas. The hydriding procedure strictly followed the pressure-composition isotherms [22] for Zr–H system. The final composition of the hydride specimen is determined as $ZrH_{1.83}$. One pure hydride sample and one Zr sample, both having a size of $2 \times 2 \times 4$ mm, were then polished and etched. X-ray diffraction shows that the majority phase in hydride specimen is ϵ -hydrides with an average grain size over 100 μm .

2.2. Nano-indentation test

The experiment is performed by Hystron's Tribo-Indenter™ using a 60° conical diamond indenter with a less than 1 μm tip radius for testing the hardness, elastic modulus, and yield stress of pure hydride and Zr samples.

To measure the hardness and reduced modulus of pure hydride and Zr, a peak load of 1000 μN is applied to the samples with the same loading and unloading

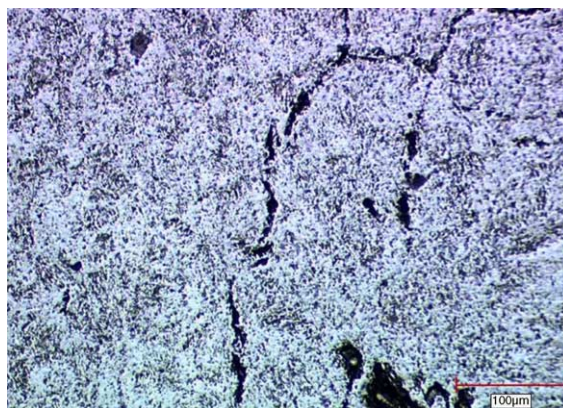


Fig. 1. Optical microscopy of pure hydride ($ZrH_{1.83}$) 150 \times .

rates of 100 $\mu\text{N/s}$. The diameter of plastic zone around an indentation mark is generally less than 5 μm , which is much less than the average grain size. Therefore, when indentation is performed at different grains, the result may be different because of the anisotropy of the grains. In addition, there are some voids (Fig. 1) in the pure hydride sample, particularly at grain boundaries. When the indenter indents into a hole or close to it, error can be introduced. Care should be taken to avoid the indentations into these voids, or the result should be disregarded. In this experiment, the indentations were made on six areas of each sample. In each area the machine was controlled to indent at 30 different positions along one straight line with a 20 μm separation between two consecutive indentations.

To measure the yield stress, an in situ atomic force microscopy (AFM) equipped with TriboIndenter was used to scan the sample surface and to search for a smooth area of at least 10 $\mu\text{m} \times 10 \mu\text{m}$. Then the indentation was made in this area at the same loading rate as in the modulus measurements. The resulting indentation marks were imaged by the in situ AFM immediately after unloading. The plastic zone boundary was taken to be the location where the pileup around the indentation marks became tangent to the flat surface. The cross-section analysis was performed on all indentation marks to measure the extent of the plastic zone. At each indent mark, four cross-sections, each at a 45° interval, were taken through the center of the mark to obtain an average plastic zone radius.

2.3. Micro-hardness tests

A micro-hardness tester with the maximum load of 1000 gf is used to indent on the hydride and Zr samples. The length of the radial cracks c was measured in situ by the micro-hardness tester to calculate the fracture toughness of the hydride.

3. Results and discussion

3.1. Hardness and reduced modulus of pure hydride and Zr

Fig. 2 is a typical load-displacement curve in nano-indentation. The reduced modulus and hardness were measured based on the method of Oliver and Pharr [23], and shown in Figs. 3 and 4, respectively. Table 1 listed the average and standard deviation of hardness and reduced modulus calculated from the data shown in Figs. 3 and 4.

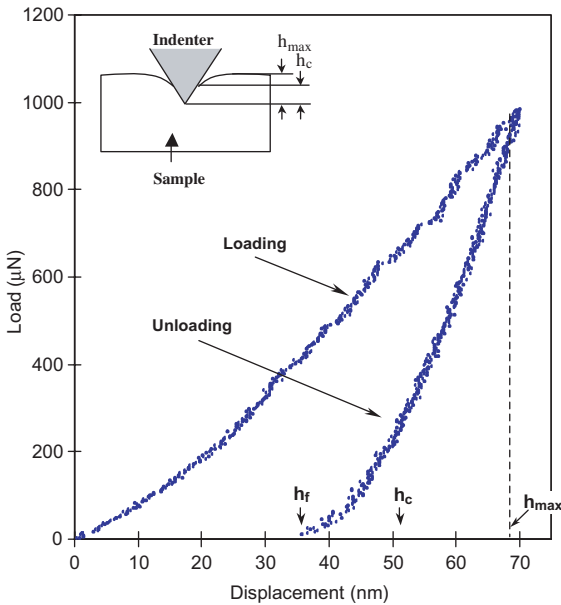


Fig. 2. Typical load-displacement curve in nano-indentation: h_f = residual depth; h_c = contact depth; h_{max} = maximum depth.

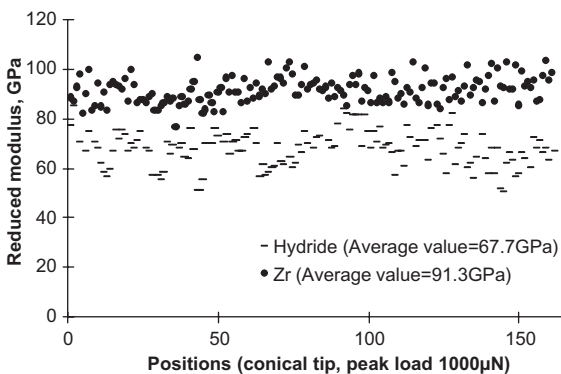


Fig. 3. Reduced modulus of Zr and hydride measured by conical diamond tip.

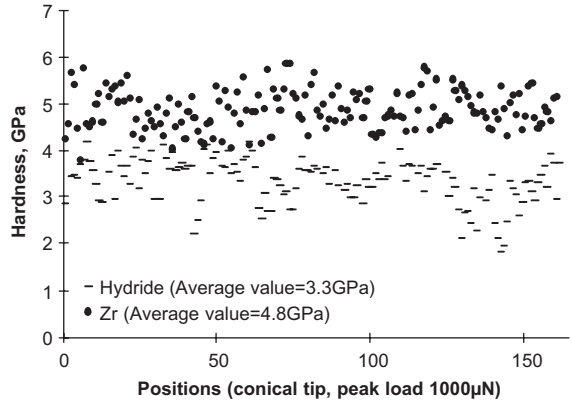


Fig. 4. Hardness of Zr and hydride measured by conical diamond tip.

The relationship between the reduced modulus (E_r) and the Young's modulus of the specimen is given by:

$$\frac{1}{E_r} = \frac{1 - \nu^2}{E} + \frac{1 - \nu_i^2}{E_i}, \quad (1)$$

where ν and E are Poisson's ratio and the elastic modulus of the specimen, respectively; and ν_i and E_i are Poisson's ratio and the elastic modulus of the diamond indenter, respectively. The elastic modulus of the indenter (E_i) is 1140 GPa, and Poisson's ratio of the indenter (ν_i) is 0.07. At room temperature, the Poisson's ratio of a Zr alloy is about 0.4 [13]. However, Poisson's ratio of the pure hydride was not reported in literature. Therefore we assume that it may take values from 0.1 to 0.4. As a result, the elastic modulus and its standard deviation for pure hydride and Zr can be calculated using Eq. (1), see Table 2. It can be seen that the elastic modulus of hydrides is lower than that for Zr by 12–25%.

3.2. Yield stress of pure hydride

The yield stress of a material, σ_y , may be determined by nano-indentation [24]

$$r = \sqrt{\frac{3P}{2\pi\sigma_y}}, \quad (2)$$

where P is the indentation load, r is the radius of the elastic–plastic boundary around the indentation mark. This model assumes that the mechanical properties of the material is isotropic, and that there is no strain hardening at the elastic–plastic boundary.

A typical indentation profile of the pure hydride sample is shown in Fig. 5, which was measured using an in situ atomic force microscopy (AFM) in TriboIndenter™. The non-symmetrical shape of the pileup region

Table 1
Reduced modulus (GPa) and hardness (GPa) of Zr and hydride indented by conical diamond tip

	Zr		Hydride	
	Reduced modulus	Hardness	Reduced modulus	Hardness
Average	91.34	4.86	67.66	3.31
Standard deviation	5.29	0.42	6.97	0.47

Table 2
Elastic modulus (GPa) of Zr and hydride indented by conical diamond tip

	Zr		Hydride		
Poisson's ratio	0.43 ^[10]	0.1	0.2	0.3	0.4
Average	80.90	71.19	69.03	65.44	60.40
Standard deviation	5.09	7.80	7.55	7.16	6.61

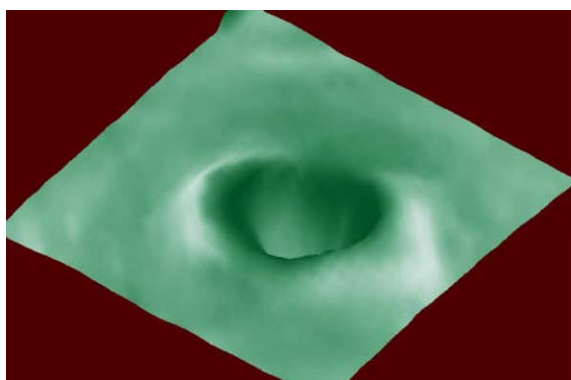


Fig. 5. AFM image of a typical nano-indentation mark on hydrides.

around the indent may be an indication of anisotropy of the grain. The position of the markers on the profile (Fig. 6) indicates the size of the plastic zone. By measuring along four different directions at 45° interval across the indentation mark, an average plastic zone radius can be obtained. The yield stress can then be calculated using Eq. (2). By varying the peak load of indentations, we found that the radius of the plastic zone size increased slowly and saturated at a load about 5000 μN. Therefore, in the measurements of yield stress, a peak load of 7000 μN was used. The average value of yield stress for the hydride sample is 478 MPa, which is about 40% below the value for Zr (780 MPa).

3.3. Fracture toughness

Fracture toughness of hydride can be conveniently measured by Vickers micro-indentation method. The measurement is based on following approximation [25]:

$$K_{IC} = \alpha \left[\frac{E}{H} \right]^{\frac{1}{2}} \left[\frac{P}{c^{\frac{3}{2}}} \right], \quad (3)$$

where K_{IC} is the fracture toughness, E is the Young's modulus of the material, H is the hardness, P is the applied load, c is the length of the radial cracks, and α is an empirical constant. This constant is a geometric function of the indenter type. For Vickers indenter α is 0.016. E and H were obtained from low load nano-indentation tests and it is assumed that these parameters are independent of load. According to the nano-indentation results, when the peak load is around 0.7 mN, the reduced modulus and hardness have reached their steady-state value. The constant c was the average value measured by an optical microscope along two directions of the Vickers indent. Fig. 7 shows a typical indentation image. The indentation peak load was 500 gf. An average fracture toughness of zirconium hydride was calculated as 0.74 MPa m^{1/2}, which is much smaller than the fracture toughness for Zr alloy (~40 MPa m^{1/2}) reported in literature.

4. Conclusions

Mechanical properties, such as hardness, Young's modulus, yield stress and fracture toughness of zirconium hydride (ZrH_{1.83}), have been measured by nano-indentation and micro-indentation techniques. Following results were observed:

- The Young's modulus of hydrides is smaller than that of Zr by 12–25%.
- The yield stress of hydrides is lower than that of Zr by about 40%.
- The fracture toughness of hydrides is about two orders of magnitude smaller than that of Zr.

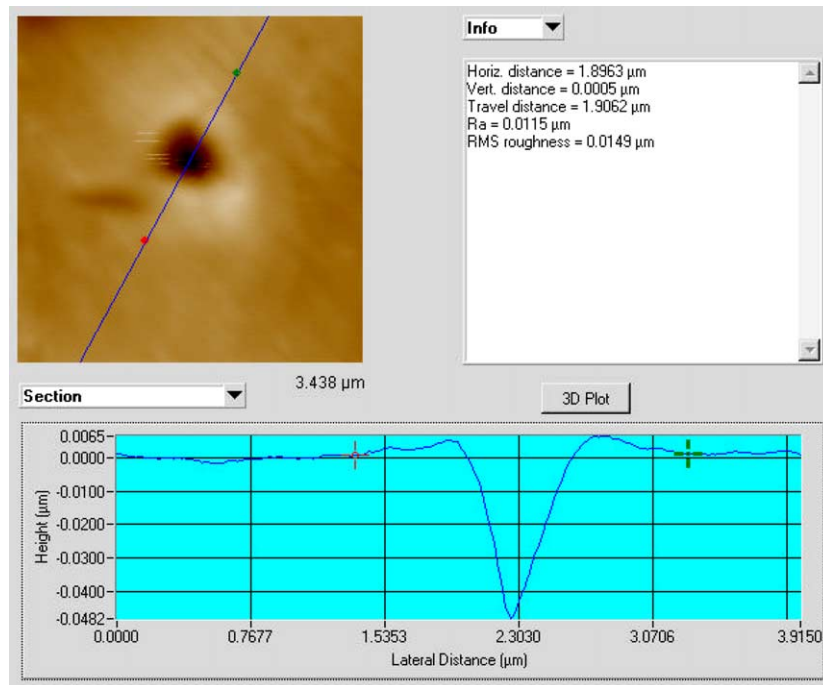


Fig. 6. AFM cross-section view of an indentation mark on pure hydride.

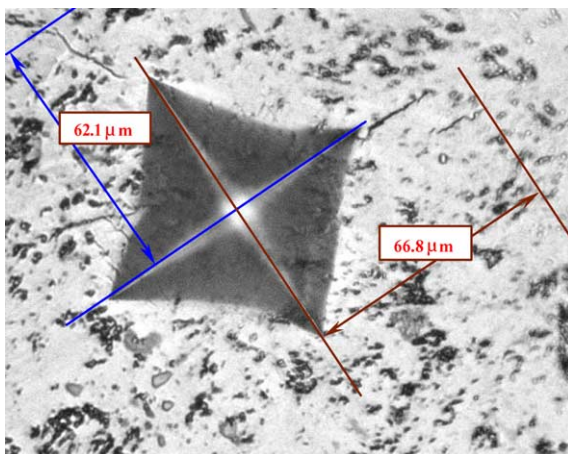


Fig. 7. Fracture toughness measurement on zirconium hydride by micro-indentation technique.

Acknowledgements

This work was funded by grants from the Research Grants Council of Hong Kong (B-Q617) and from the Hong Kong Polytechnic University (G-T443).

References

- [1] R.L. Beck, W.M. Mueller, in: W.H. Mueller et al. (Eds.), *Metal Hydrides*, Academic Press, New York, 1968, p. 312.
- [2] K.G. Barraclough, C.J. Beevers, *J. Mater. Sci.* 4 (1969) 518.
- [3] C.J. Beevers, K.G. Barraclough, *J. Mater. Sci.* 4 (1969) 802.
- [4] J.F.R. Ambler, Atomic Energy of Canada, Report, AECL-2538, 1966.
- [5] L.A. Simpson, K. Nuttall, ASTM STP 633 (1977) 608.
- [6] R. Dutton, K. Nuttall, M.P. Puls, L.A. Simpson, *Metall. Trans.* 8A (1977) 1553.
- [7] L.A. Simpson, M.P. Puls, *Met. Trans. A* 10A (1979) 1093.
- [8] L.A. Simpson, C.D. Cann, *J. Nucl. Mater.* 87 (1979) 303.
- [9] S.Q. Shi, M.P. Puls, *J. Nucl. Mater.* 275 (1999) 312.
- [10] S. Yamanaka, K. Yoshioka, M. Uno, M. Katsura, H. Anada, T. Matsuda, S. Kobayashi, *J. Alloys Compd.* 293–295 (1999) 23.
- [11] S. Yamanaka, K. Yoshioka, M. Uno, M. Katsura, H. Anada, T. Matsuda, S. Kobayashi, *J. Alloys Compd.* 293–295 (1999) 908.
- [12] S.Q. Shi, M.P. Puls, unpublished research, AECL, 1995.
- [13] S.Q. Shi, M.P. Puls, *J. Nucl. Mater.* 208 (1994) 232.
- [14] S.Q. Shi, M.P. Puls, S. Sagat, *J. Nucl. Mater.* 208 (1994) 243.
- [15] E. Smith, *Int. J. Pressure Vessels Piping* 60 (1994) 159.
- [16] X.J. Zheng, L. Luo, D.R. Metzger, R.G. Sauve, A Unified Model of Hydride Cracking Based on Elasto-Plastic

- Energy Release Rate over A Finite Crack Extension, Ontario Hydro Technologies Report No. B-NFC-94-46-K, Toronto, Canada, 1994.
- [17] S.Q. Shi, M.P. Puls, in: A.W. Thompson, N.R. Moody (Eds.), *Hydrogen Effects in Materials*, TMS, 1996, p. 611.
- [18] J. Lufrano, P. Sofronis, H.K. Birnbaum, *J. Mech. Phys. Solids* 44 (2) (1996) 179.
- [19] Y.S. Kim, Y.G. Matvienko, Y.M. Cheong, S.S. Kim, S.C. Kwon, *J. Nucl. Mater.* 278 (2000) 251.
- [20] A.G. Varias, A.R. Massih, *J. Nucl. Mater.* 279 (2000) 273.
- [21] J.D. Eshelby, *Proc. R. Soc. A* 241 (1957) 376.
- [22] L.A. Simpson, C.D. Cann, *J. Nucl. Mater.* 87 (1979) 302.
- [23] W.C. Oliver, G.M. Pharr, *J. Mater. Res.* 7 (6) (1992) 1564.
- [24] J.S. Robach, *Mater. Res. Soc. Symp. Proc.* 522 (1998) 133.
- [25] L. Riestler, R.J. Bridge, K. Breder, *Mater. Res. Soc. Symp. Proc.* 522 (1998) 45.